

Light scattering by a nanoparticle and a dipole placed near a dielectric surface covered by a thin metallic film

Pavel I. Geshev^{*1}, Ulrich C. Fischer² and Harald Fuchs²

¹*Institute of Thermophysics of the Russian Academy of Sciences, Lavrentyev Ave., 1, and Novosibirsk State University, Pirogova Str., 2, Novosibirsk, 630090, Russia*

²*Westfälische Wilhelms-Universität, Wilhelm-Klemm-Str. 10, Münster, 48149, Germany*
Geshev@itp.nsc.ru

Abstract: On the basis of Maxwell's equations a light scattering system of axial symmetry is considered, which consists of a nanoparticle, a dipole and a metal film (covering a dielectric support). Nanoparticle (NP) and dipole are situated on an axis of symmetry and the dipole is oriented along the axis and placed between film and nanoparticle. The field enhancement factor F and dipole energy flux D are calculated by the Green's function method: the initial system of Maxwell's equations is reduced to a system of boundary integral equations, and solutions are obtained by the boundary element method. Illumination of the scattering system by a radially polarized Bessel light beam causes a field enhancement in the vicinity of the film surface. The metallic NP closely placed at the film surface acts as nano-antenna. Surface plasmons excited in the particle and film convert the incident propagating EM field into non-propagating evanescent near-field. Then the field is confined and strongly enhanced in a particle/film gap. The enhancement of Raman radiation depends on many factors: size and shape of NP, permittivities of all materials, light wavelength, film thickness, angle of light beam, and - very strongly - on the gap distance. The field enhancement in a gap ~ 1 nm can be 10^3 and more and the Raman radiation enhancement factor can reach huge values $\sim 10^{10}$ - 10^{12} . Whereas for small nanoparticles the field enhancement factor F and the dipole energy flux D do not depend on the direction of the exciting beam and on the angle of emission, a strong influence is found for extended particles. This influence is plausibly explained by a larger overlap between the electric field of the exciting beam or the emitted radiation field with the near field distribution of the nanoparticle leading to higher F and D values, respectively.

©2007 Optical Society of America

OCIS codes: (240.0310) Thin films; (240.6680) Surface plasmons; (260.6970) Total internal reflection; (290.5850) Scattering, particle; (240.0310) Scattering, Raman

References and Links

1. D. L. Jeanmaire and R. P. Van Duyne, "Surface Raman spectroelectrochemistry. Part I. Heterocyclic, aromatic, and aliphatic amines adsorbed on the anodized silver electrode," *J. Electroanal. Chem.* **84**, 1 (1977).
2. M. Moskovits, "Surface-enhanced spectroscopy," *Rev. Mod. Phys.*, **57**, N.3, 783 (1985).
3. K. Kneipp, Y. Wang, H. Kneipp, L. T. Perelman, I. Itzkan, R. Dasari, and M. S. Feld, "Single molecule detection using Surface-Enhanced Raman Scattering (SERS)," *Phys. Rev. Lett.* **78**, 1667 (1997).
4. S. M. Nie and S. R. Emory, "Probing single molecules and single nanoparticles by Surface Enhanced Raman Scattering," *Science* **275**, 1102 (1997).
5. H. Xu, E. J. Bjerneld, M. Käll, and L. Börjesson, "Spectroscopy of single hemoglobin molecules by Surface Enhanced Raman Scattering," *Phys. Rev. Lett.* **83**, 4357 (1999).
6. A.M. Michaels, M. Nirmal, and L.E. Brus, "Surface Enhanced Raman Spectroscopy of individual rhodamine 6G molecules on large Ag nanocrystals," *J. Am. Chem. Soc.* **121**, 9932 (1999).
7. J. Wessel, "Surface-enhanced optical microscopy," *J. Opt. Soc. Am. B* **2**, 1538 (1985).

8. U. C. Fischer and D. W. Pohl, "Observation of single-particle plasmons by near-field optical microscopy," *Phys. Rev. Lett.* **62**, 458 (1989).
9. Y. Inouye and S. Kawata, "Near-field scanning optical microscope with a metallic probe tip," *Opt. Lett.* **19**(3), 159 (1994).
10. M. Inoue and K. Ohtaka, "Surface Enhanced Raman Scattering by metal spheres. I. Cluster effect," *Phys. Soc. Japan* **52**, 3853 (1983).
11. T. Takemori, M. Inoue, and K. Ohtaka, "Optical response of a sphere coupled to a metal substrate," *J. Phys. Soc. Japan* **56**, 1587 (1987).
12. M. S. Anderson, "Locally enhanced Raman spectroscopy with an atomic force microscope," *Appl. Phys. Lett.* **76**, 3130 (2000).
13. R. M. Stöckle, Y. D. Suh, V. Deckert, and R. Zenobi, "Nanoscale chemical analysis by tip-enhanced Raman microscopy," *Chem. Phys. Lett.* **318**, 131 (2000).
14. N. Hayazawa, A. Tarun, Y. Inouye, and S. Kawata, "Near-field enhanced Raman spectroscopy using side illumination optics," *J. Appl. Phys.* **92**, 6983 (2002).
15. B. Pettinger, B. Ren, G. Picardi, R. Schuster, and G. Ertl, "Tip-enhanced Raman spectroscopy (TERS) of malachite green isothiocyanate at Au(111): bleaching behavior under the influence of high electromagnetic fields," *J. Raman Spectrosc.* **36**, 541, (2005).
16. K. Li, M.I. Stockman, and D.J. Bergman, "Self-similar chain of metal nanospheres as an efficient nanolens," *Phys. Rev. Lett.* **91**, 227402 (2003).
17. M. Futamata, Y. Maruyama, and M. Ishikawa, "Local electric field and scattering cross section of Ag nanoparticles under surface plasmon resonance by finite difference time domain method," *J. Phys. Chem. B* **107**, 7607 (2003).
18. A. Downes, D. Salter, and A. Elfick, "Heating effects in tip-enhanced optical microscopy," *Opt. Express* **14**, 5216 (2006).
19. P. I. Geshev, S. Klein, T. Witting, K. Dickmann, and M. Hietschold, "Calculation of the electric-field enhancement at nanoparticles of arbitrary shape in close proximity to a metallic surface," *Phys. Rev. B* **70**, 075402 (2004).
20. P.I. Geshev and K. Dickmann, "Enhanced radiation of a dipole placed between a metallic surface and a nanoparticle," *J. Opt. A: Pure Appl. Opt.* **8**, S161 (2006).
21. A. Sommerfeld, "Partial differential equations in physics," Academic Press, New-York, 1967.
22. F.J. Garcia de Abajo and A. Howie, "Retarded field calculation of electron energy loss in inhomogeneous dielectrics," *Phys. Rev. B* **65**, 115418 (2002).
23. J. Aizpurua, G.W. Bryant, L.J. Richter, and F.J. Garcia de Abajo, "Optical properties of coupled metallic nanorods for field-enhanced spectroscopy," *Phys. Rev. B* **71**, 235420 (2005).
24. E. Kretschmann, "Die Bestimmung optischer Konstanten von Metallen durch Anregung von Oberflächenplasmaschwingungen," *Z. Physik*, **241**, 313 (1971).
25. L. Novotny, M.R. Beversluis, K.S. Youngworth, and T.G. Brown, "Longitudinal field modes probed by single molecules," *Phys. Rev. Lett.* **86**, 5251 (2001).
26. T. Grosjean, D. Courjon, and D. Van Labeke, "Bessel beams as virtual tips for near-field optics," *J. Microsc.* **210**, 319-323 (2003).
27. K. Sakoda, K. Ohtaka, and E. Hanamura, "Surface Enhanced Raman Scattering in attenuated total reflection arrangement," *Solid State Comm.* **41**, 393 (1982).
28. B. Pettinger, A. Tadjeddine, and D.M. Kolb, "Enhancement in Raman intensity by use of surface plasmons," *Chem. Phys. Lett.* **66**, 544 (1979).
29. P.B. Johnson and R.W. Christy, "Optical constants of the noble metals," *Phys. Rev. B* **6**, 4370 (1972).
30. A. Otto, "On the electronic contribution to single molecule surface enhanced Raman spectroscopy," *Indian J. Phys.* **77 B** (1), 63 (2003).
31. L.D. Landau and E.M. Lifschiz, "Elektrodynamik der Kontinua," Akademi-Verlag, Berlin, 1974.
32. E.C. Le Ru and P.G. Etchegoin, "Rigorous justification of the $|E|^4$ enhancement factor in Surface Enhanced Raman Spectroscopy," *Chem. Phys. Lett.* **423**, 63 (2006).
33. L. Novotny, and B. Hecht, "Principles of Nano-Optics," Cambridge University Press, New York, 2006.
34. P. Johansson, "Light emission from a scanning tunneling microscope: Fully retarded calculation," *Phys. Rev. B* **58**, 10823 (1998).
35. E.I. Ibragimov and A.G. Malshukov, "Landau damping of plasma oscillations localized near a STM tip apex," *Optics and Spectroscopy* **76**, N.2, 350 (1994).

1. Introduction

Enhancement factors for Raman radiation of molecules adsorbed on rough metallic surfaces reach values $\sim 10^6$ - 10^7 (phenomenon known as surface enhanced Raman scattering, SERS, [1, 2]). For molecules adsorbed on silver and gold nanoparticles in colloids it is found that the Raman radiation is enhanced enormously: up to $\sim 10^{14}$ times according Kneipp et al. and Nie and Emory [3, 4]. This phenomenon was explained by Xu et al. and by Michaels et al. [5, 6]

as effect of field confinement in the gap between two closely placed nanoparticles, where a Raman radiating molecule is trapped. Due to this huge enhancement factor one can speak about single molecule surface enhanced Raman scattering (SM-SERS).

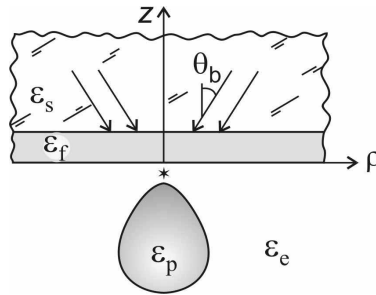


Fig. 1. Light scattering system.

Another nano-object which can be considered as nanoparticle (NP) is the tip of a scanning tunneling microscope (STM) or an atomic force microscope (AFM). The radii of curvature R_c of these tips are in the order of 10-100 nm. The idea to use a metallic NP for detection of surface features by Raman signals was suggested by Wessel [7]. Realization of this idea in experiments with elastic light scattering on a spherical metallic nanoshell [8] and metallic tip [9] have shown a large increase of scattered energy with decreasing gap size. First calculations of light scattering on a system Ag sphere/ Ag surface also have shown an increase of the Raman signal by a factor $\sim 10^8$, [10, 11].

Recent experiments [12-15] have been devoted to tip enhanced Raman scattering (TERS). In this case an illuminated STM or AFM tip is used to enhance the Raman signal. The largest estimated Raman radiation enhancement factor (*REF*) in these experiments is $6 \cdot 10^6$, [15]. This value is less by 6-7 orders of magnitude than corresponding *REF* for SM-SERS, [3, 4]. Due to a similarity in electromagnetic mechanisms of SERS and TERS one should expect similar values for *REF* in SM-TERS and SM-SERS. Because STM and AFM devices are among the major tools used for investigation on the nanolevel it is important to estimate the potential of TERS in a sense of single molecule spectroscopy.

The aim of our article is the determination of an efficiency of a metallic NP as a receiving and radiating nano-antenna: the nanoparticle's enhancement factors for received (F^2) and radiated (D) signals are introduced and calculated. The total *REF* is proportional to the product $F^2 D$. Recently, numerically calculated *REF* $\sim 10^{10}$ - 10^{12} were announced for clusters of metallic nanospheres or for metallic tip / metallic surface configurations at gaps $g \sim 1$ nm, [16-18]. It is in accordance with a previously obtained result [5], and with *REF* calculated in papers [19, 20]. Li et al. [16] considered a self-similar chain of metallic nanospheres and found in the gap between the smallest spheres of diameter 5 nm the enhancement factor higher than 10^{12} . They used in the non-retardation approach a method of decomposition of the solution over a set of spherical harmonics. Futamata et al. [17], have calculated an enhancement factor of order of *REF* $\sim 10^{10}$ - 10^{11} for two closely placed (1 nm) Ag nanoparticles. They used the finite difference time domain method. Downes et al. [18], used finite element method and calculated electromagnetic and temperature fields in and around an STM (AFM) tip in proximity to a metallic support illuminated from the side. They obtained *REF* $> 10^{10}$ for the *p*-polarized beam and for a gap distance ~ 1 nm.

In the present article we will expand the previously developed method of calculation of axially symmetrical solutions of Maxwell equations, [19, 20], to the layered medium (metallic film on a dielectric support). The boundary element method (BEM), used in [19, 20], is faster and more robust than the methods described above, [16-18]. We could calculate detailed results for a wide spectral region (200 discrete photon energies in the visible and infra-red).

The paper is organized as follows: In section 2 a short description of BEM and Bessel beam is given; in section 3 the enhancement effect of the metallic film is considered; in section 4 the main results for the NP enhancement effect are described and section 5 contains the conclusions.

2. Setting of the problem and method of solution. The Bessel light beam

Let's consider a dipole (oriented along the z -axis) and a NP placed close to a surface of a metallic film, deposited on a dielectric support (Fig. 1). Permittivities of support (ϵ_s) and environment (ϵ_e) are real and positive. Permittivities of the metallic film (ϵ_f) and the nanoparticle (ϵ_p) are complex functions of light frequency. Calculations are based on Maxwell's equations applied to the axially symmetric scattering system shown in Fig. 1. Maxwell's equations are reduced to a system of two integral equations with unknown boundary values of the tangential component of the magnetic field (H_ϕ) and its normal derivative ($H_\phi' = \partial H_\phi / \partial n$). Discretization of the system of integral equations in the boundary element method leads to a system of linear algebraic equations for H_ϕ and H_ϕ' , taken on a contour of NP. A solution of this system can be obtained by the regular Gauss method. It gives values H_ϕ and H_ϕ' on a NP contour. The full electromagnetic field inside and outside the NP is then represented by the known Green formula [19, 20].

For the case considered previously (empty and metallic semi-spaces, [19, 20]) the kernel functions in the integral equations were the Green's functions of the vector Helmholtz equations, expressed via the Sommerfeld integrals [21]. In the present paper the Green's function method [19, 20] is expanded to the case of a layered medium (thin metallic film placed between two dielectric semi-spaces).

The boundary element method is widely used in computational electrodynamics (see e.g. papers devoted to light scattering on a cluster of nanoparticles [22, 23]). But usually, the complex impact of the layered medium is not taken into account.

The motivation to consider a metallic film is caused by the Kretschmann configuration [24], frequently used in experiments. The illumination can be applied through the dielectric support and the film from above (beam angle is positive, $\theta > 0$) or from the environment region, from below ($\theta < 0$). A total internal reflection occurs for $\theta > \theta_{cr}$, where $\theta_{cr} = \text{Sin}^{-1}(\sqrt{\epsilon_e / \epsilon_s})$. This configuration is introduced by Kretschmann [24] for exciting strong plasmon oscillations in a metallic film (attenuated total reflection, ATR). We use a radial polarized Bessel beam (BB), considered also by Novotny et al. and Grosjean et al. [25, 26]. Another light source is a dipole. We use the dipole field [20], generalized here to the case of a dipole near a thin metallic film, as it is done also by Sakoda et al. [27].

The use of BB instead of a plane wave can be explained as follows: The z -component of the electric field in a plane p -polarized EM wave, reflected from a layered medium, can be represented also in cylindrical coordinates:

$$E_z = E_0 \sin \theta \left[e^{i\mathbf{k}\mathbf{x}} + R(\theta) e^{i\mathbf{k}'\mathbf{x}} \right] = E_0 \sin \theta \left[e^{ikz \cos \theta} + R(\theta) e^{-ikz \cos \theta} \right] \cdot \left[J_0(k\rho \sin \theta) + 2 \sum_{n=0}^{\infty} J_n(k\rho \sin \theta) i^n \cos n(\varphi - \psi) \right]$$

where E_0 is an amplitude in the plane wave, coordinates z, ρ, ψ indicate an observation point (\mathbf{x}), a wave vector \mathbf{k} has angles in spherical coordinates φ and θ and length $k = \epsilon^{1/2} \omega / c$, where ω is the light frequency and c is the light velocity. The two terms in the first square brackets represent the incident and reflected waves, respectively. The second vector \mathbf{k}' has the same angle φ and a reflected angle $\pi - \theta$. The reflection coefficient $R(\theta)$ depends on the parameters: angle θ , all permittivities ϵ_i and film thickness h . From this formula we conclude that on a z -axis (at $\rho = 0$) the contribution to the field E_z comes only from the first term in the second square brackets (the Bessel function of zero order). This term describes the radial polarized Bessel light beam. Therefore, for our aims - calculation of enhancement factors for the local

field and for the dipole radiation - it is sufficient to use the model with axial symmetric illumination sources (BB and dipole).

3. Film enhancement factors

The main calculated values are the enhanced electric field $E(z_0, g)$, taken at the dipole position, and the dipole radiation flux $j(z_0, g)$, depending on the dipole coordinate z_0 and on the NP/film gap g . At first the system without nanoparticle is considered, that means $g=\infty$. To characterize the film impact on the field enhancement and on the dipole radiation the next four dimensionless factors are introduced:

$$A_+ = E_+(z_0, \infty) / E_0; \quad A_- = E_-(z_0, \infty) / E_0; \quad J_+ = j_+(z_0, \infty) / j_0; \quad J_- = j_-(z_0, \infty) / j_0,$$

where E_0 is the electric field in the incident wave, j_0 is the semi-flux from the dipole in empty space. Two signs + and - designate the upper and lower semi-spaces from which the EM waves can illuminate the scattering system and the directions to which the enhanced Raman radiation is radiated (see Fig. 1). We obtain J_+ and J_- by integration of the Poynting vector over planes situated above or below the film and the dipole, respectively (see details in [20]).

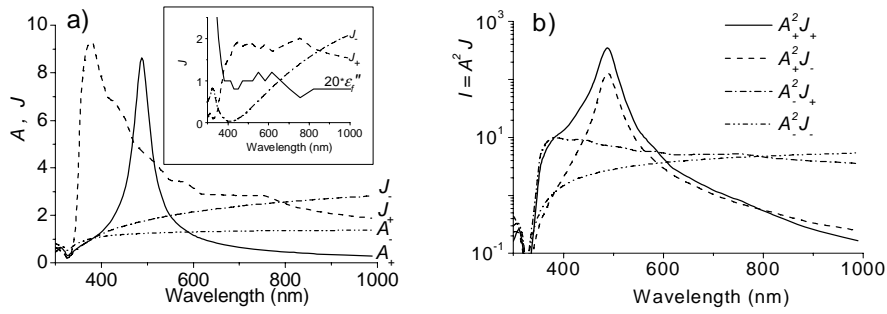


Fig. 2. (a) Film amplification factors for electric field (A) and for dipole energy flux (J); (b) Raman radiation enhancement factor I describing the effect of metallic film.

In Fig. 2(a) the values A for beam angles 45° (A_+) and -45° (A_-), are shown, respectively. The optimal choice of the film thickness is $h = 50$ nm: plasmons in an Ag film have maximal amplitudes at this value of h , [27, 28]. Dimensionless dipole energy fluxes J radiated into the dielectric support (J_+) or into the environment (J_-) are shown in Fig. 2(a) for dipole distance $z_0 = -0.5$ nm. Some disturbances on the curve for J_+ are connected with experimental errors in the imaginary part of metal permittivity, $\epsilon_f'' = \text{Im}(\epsilon_f)$, taken from Johnson and Christy [29] for Ag. In the inset of Fig. 2(a) the enlarged value of ϵ_f'' is compared with the fluxes J_+ and J_- calculated for the dipole position $z_0 = -100$ nm and a strong correlation between values ϵ_f'' and J_+ is seen. Note, that the disturbances in ϵ_f'' have no strong influence on the reflected flux J_- (see inset in Fig. 2(a)).

One can obtain an expression for the film amplification factor A_+ :

$$A_+ = \frac{\left| \frac{(1 - \Lambda_{ef})(1 + \Lambda_{sf}) \exp[i(\chi_f - \chi_s)h - i\chi_e z_0]}{1 - \Lambda_{ef}\Lambda_{sf} \exp(2i\chi_f h)} \right| \sqrt{\epsilon_s} \sin \theta}{\epsilon_e}$$

$$\Lambda_{ij} = \frac{\chi_i \epsilon_i - \chi_j \epsilon_i}{\chi_i \epsilon_j + \chi_j \epsilon_i}; \quad \chi_i = \sqrt{\epsilon_i - \epsilon_s \sin^2 \theta}; \quad (i, j = e, f, s).$$

The surface plasmons excited in the film by BB at ATR conditions produce a maximal value of the z -component of electric field at the central point ($\rho=0$; $z=0$; Fig. 1). For relatively

thick films ($h > 40$ nm) one can obtain from A_+ an approximate formula connecting the beam angle and the resonant plasmon frequency ω_{res}

$$\sin \theta = \text{Re} \left(\frac{\epsilon_s + \frac{\epsilon_s}{\epsilon_f(\omega_{res})}}{\epsilon_e} \right)^{-\frac{1}{2}}$$

For the air/glass interface the critical angle is $\theta_{cr} = 41.81^\circ$. For decreasing angles less than 42.5° the resonant frequency of the surface plasmon is shifting to the infrared.

As a measure of the film impact on the dipole Raman radiation one can introduce the total intensity enhancement factor $I = A^2 J$. There exist four combinations of values A^2 and J in the value I . All these factors I are calculated for the same parameters and shown in Fig. 2(b). Note that the maximal value of I for the Raman signal radiated from a system dipole/film is about few hundreds. It is not very much and is in accordance with the known fact: there is no large SERS effect on flat metallic surfaces [2, 28].

4. Nanoparticle enhancement factors

When a NP is present the problem of calculation of the total Raman radiation enhancement factor is decomposed into two parts: a) calculation of the field enhancement factor (FEF), that is the enhanced electric field calculated at the dipole position, divided by the field in the incident wave: $FEF = E(z_0, g) / E_0$; b) calculation of the dimensionless dipole energy flux (DEF), enhanced due to the presence of NP: $DEF = j(z_0, g) / j_0$. DEF is obtained by integration of z -component of the Poynting vector over the planes placed above and below the scattering system shown in Fig. 1. The semi-flux j_0 of a free dipole is used to make DEF dimensionless.

The most relevant measures of the effect of the NP in TERS are the relative enhancement factors introduced by the ratios: $F = FEF/A$, and $D = DEF/J$. These factors become equal to one for very far retraction of a NP from the film. There are two factors F_+ and F_- for two directions of illumination ($\theta > 0$ and $\theta < 0$), and two factors D_+ and D_- for positive and negative directions of the dipole radiation with respect to the z -axis. The total Raman enhancement factor (REF) is determined as the product: $REF = I F^2 D$. There are four combinations for two incident and two radiated EM waves indicated in subscripts of the introduced factors. In values REF and I the first sign in the subscript refers to the direction from which the EM wave comes, the second one indicates the direction of the radiated Raman signal.

In Fig. 3 the relative field enhancement factors F for a silver sphere at the sphere's poles situated *close* and *far* from the film surface are shown vs. the gap distance g . The value F_{CLOSE} seems to be proportional to $g^{-4/3}$ (average trend). It is a stronger dependence than the one can be expected from a simple electrostatic nanocapacitor model ($FEF \sim g^{-1}$). Plasmon resonances are clearly seen for the factor F_{FAR} (insets, Fig. 3). For different silver spheres having diameters 50 and 100 nm the light wavelengths are chosen such, that the first dipole plasmon resonance occurs at $g = 1$ nm.

A quantum effect can change the huge calculated REF , shown in Fig. 3 for small gaps ($g < 0.5$ nm). It is the electronic tunneling between the NP and metallic film, which must decrease the electric field confined in the gap (see Otto [30]).

In Fig. 4(a) for a silver sphere of diameter $d = 100$ nm, the relative factors F^2 and D are compared and it becomes clear that they all have very similar values. It is a consequence of the relative definition of these factors and of the small NP size. In Fig. 4(b) values REF_{++} for ATR and REF_{-+} for non-ATR conditions are demonstrated. From Fig. 4(b) follows: 1) the maximal REF s are larger for ATR than for non-ATR conditions; 2) decreasing of the BB angle at ATR conditions shifts the maximum of REF to the red and infrared; 3) REF s maxima can reach values $\sim 10^{11}$ - 10^{12} .

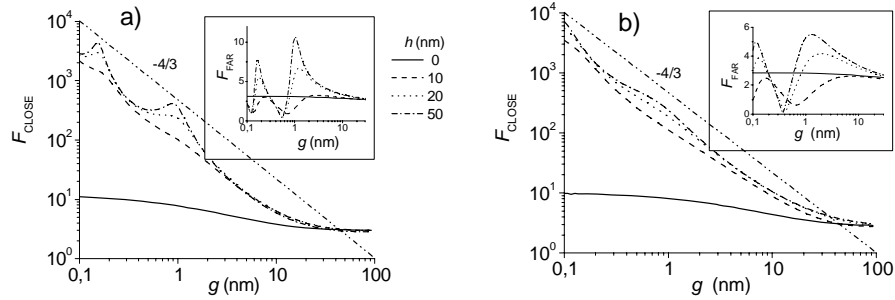


Fig. 3. Relative field enhancement factors F_{CLOSE} and F_{FAR} (insets) vs. gap distance g : a) Ag sphere $d = 50$ nm; light wavelength $\lambda=510$ nm; b) Ag sphere $d = 100$ nm; $\lambda=660$ nm. Film thicknesses are $h=0, 10, 20, 50$ nm; BB angle is $\theta=44^\circ$.

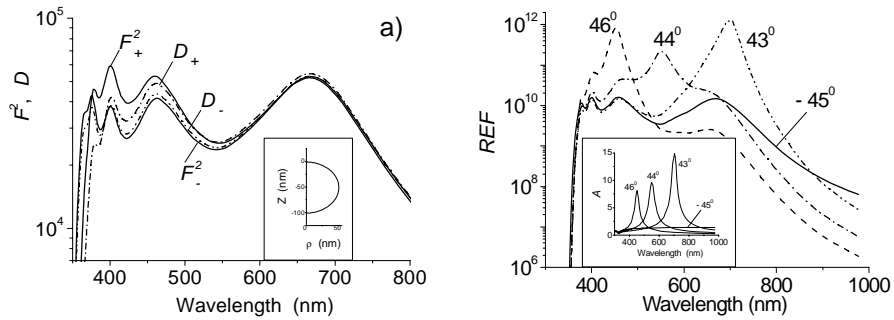


Fig. 4. Enhancement factors vs. light wavelength: a) Comparison of F^2 and D factors (inset, Ag sphere $d=100$ nm, $g=1$ nm); b) REF_{++} for BB angles $\theta=43^\circ, 44^\circ, 46^\circ$ (ATR), and REF_{+} for non-ATR angle -45° (in the inset the film factor A is shown). Dipole position is $z_0=-0.5$ nm.

It is interesting that the maxima of calculated REF remain still less than the value 10^{14} obtained in SM-SERS experiments [3, 4]. It means there is an additional chemical (quantum) enhancement mechanism, discussed by Otto, [30]. The dynamic charge transfer mechanism is the resonant electron tunneling via the orbitals of the molecule trapped in the narrow gap between two metallic electrodes [30]. It determines the SM-SERS selection rules: some adsorbed molecules produce a strong Raman signal, but vibrating molecules of other types (with no appropriate orbitals) show no signal. This effect can add two or three orders to the calculated electromagnetic REF [30].

In Fig. 5 the relative enhancement factors for three NPs having non spherical shapes are depicted vs. photon's energy expressed in electron-volt. This representation shows the calculated factors more clearly in the short wavelength region. Again, the gap distance is $g=1$ nm, and dipole position is $z_0=-0.5$ nm. Note that for Fig. 5(a,b,c) beam angles are $\pm 45^\circ$. One of them, $+45^\circ$, corresponds to ATR conditions. For Fig. 5(d) the beam angles are $\pm 40^\circ$ (both non-ATR). The spheroid's sizes, radii and vertical lengths (in nm) are: a) 144, 49; b) 70, 210; c) and d) 100, 500, respectively. Curvature radii at the very tips have values (in nm): 216 (a); 10 (b); 1 (c, d), respectively. One can see that in the high energy region the two groups of factors have an opposite tendency: the factors F_-^2 and D_- are increasing, but the values F_+^2 and D_+ are decreasing. The relative factors F^2 and D are approximately equal for the first dipole-like plasmon resonances at low photon energy. In this case, a NP acts as a dipole and corresponds more closely to conditions of the "optical reciprocity theorem" (ORT), [31, 32]. ORT in its classic form links the electric fields produced by two dipoles at the dipole positions [31]. Le Ru and Etchegoin [32] generalize ORT to the case when the second dipole is replaced

by a plane wave. They apply ORT to SERS and show that for some circumstances the frequently used law $REF \sim |E|^4$ is really fulfilled. To apply ORT it is important to have two identical light ways: from one source to another and back. This condition is not exactly fulfilled in our situation, because we do not calculate the energy returned with the light beam at the same angle but the total amount of energy crossing the control planes. Therefore, we can expect only qualitative correlations $F_+^2 \approx D_+$, $F_-^2 \approx D_-$, seen in Fig. 5(a,b,c), and not exact equalities.

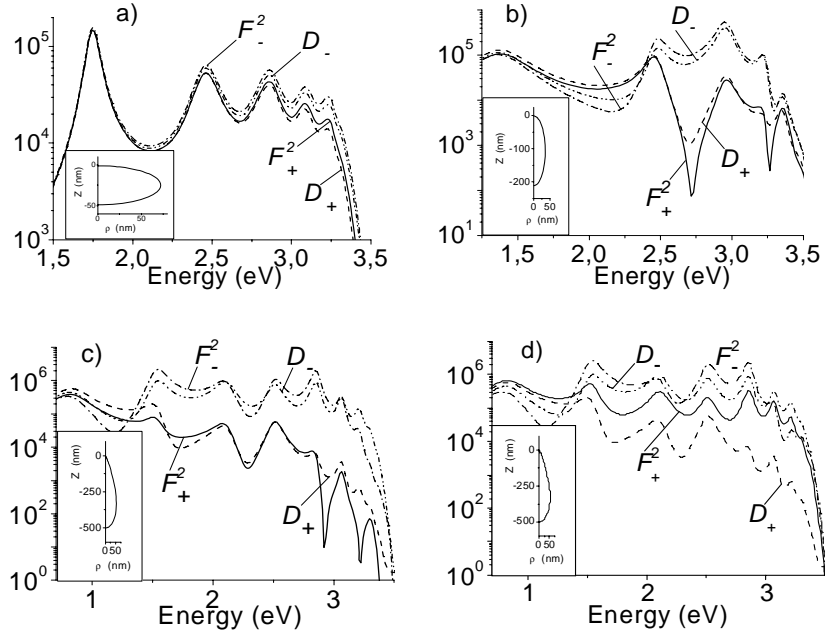


Fig. 5. Relative enhancement factors vs. photon's energy for: a) oblate spheroid; b) prolate spheroid; c) long NP with a tip radius of curvature $R_c \sim 1$ nm; d) the same NP as in (c), but for non-ATR angle of light illumination. Note the behavior of solid lines (F_+^2) in cases (c) and (d). BB angles for figures (a), (b), (c) are $\pm 45^\circ$, for figure (d) the angle is $\pm 40^\circ$.

For the case shown in Fig. 5(d), however, the factor F_+^2 is considerably larger than the factor D_+ . At the illumination angle 40° there is a non-decaying electric field in the lower subspace, where NP is placed. So, we can link the decrease of the factor F_+^2 in the short wavelength region of spectrum with a strong exponential decay of the evanescent non-propagating field. The shorter the wavelength, the stronger is the exponential decay of the field (ATR) and the lower is the contribution of the distant parts of the nanobody to the field enhancement at the dipole position. The decrease of the factor D_+ with decreasing wavelength can be explained in the following way by the exponential decay with the z -coordinate of the emission of a dipolar light source into the angular range of the so called "forbidden" part of light [33]. For the calculation of D_+ we assumed a dipolar source in the gap between nanoparticle and the surface. This dipole leads to a collective excitation of the nanoparticle, which can be considered as a distribution of dipolar sources over the surface of the nanoparticles. Only a small fraction of these distributed dipoles are within the range of the evanescent modes which are mainly responsible for the D_+ radiation. On the other hand all these dipoles can effectively contribute to the D_- radiation. Therefore, for an extended particle the D_- radiation dominates. We conclude that the values of $F_{+/-}$ and $D_{+/-}$ increase with an increasing overlap of the field of the exciting or of the emitted beam of light, respectively, with the near field of the nanoparticle.

In the case of very sharp NPs ($R_c \sim 1$ nm) and very small gaps ($g = 0.1-0.5$ nm) there is an additional mechanism which reduces the *REFs*, the Landau damping, which is connected with dissipation of plasmon's energy due to a creation of electron-hole pairs. It is a phenomenon that can not be described in the classical frame used here. It needs a quantum mechanical consideration [34, 35]. Due to the Landau damping in the case of a very sharp tip and narrow gap one can lose an order of magnitude or more in the Raman enhancement factor as estimated previously [20].

5. Conclusion

The metallic film illuminated at ATR conditions by a radially polarized Bessel light beam produces an enhanced electromagnetic evanescent field in the vicinity of the film surface. For a given angle of illumination there exists a certain resonant light frequency at which the field amplified at the silver film surface is enhanced about ten times. By a small variation of the illumination angle this maximum can scan the visible and infrared. The dipole radiation in the far field zone is also enhanced due to excitation of surface plasmons in the metallic film.

In the presence of a nanoparticle the field enhancement can reach 10^3 and more for a small gap and radius of curvature ~ 1 nm of the tip. Relative intensity enhancement factors F^2 and D can have values $\sim 10^5$ (up to 10^6 for very sharp tips). For NP shorter than Rayleigh scale ($\lambda/2\pi$) all introduced relative enhancement factors (F^2 , D) have similar values. This similarity can be connected with the relative form of these factors. But a full understanding of this fact can only be obtained by a detailed analysis of the angular distribution of the radiated light. This analysis is in progress.

In the sense of the introduced relative enhancement factors (F , D), the Kretschmann configuration responsible for F_+ and its inverse configuration of a dipole radiating into the 'forbidden' angles, being responsible for D_+ , has a disadvantage for elongated NP. This is connected with an exponentially decaying factor which decreases the contribution of distant parts of the NP to the enhanced field at the dipole position (F_+). A similar exponentially decaying factor decreases the contribution of distant parts of the NP to the radiation into the 'forbidden' angular sector above the film (a part of D_+).

The total Raman radiation enhancement factor (*REF*) is the product of the film enhancement factor (I) and the introduced relative factors: $REF = IF^2D$. The maximum of *REF* can reach values $\sim 10^{10}-10^{12}$. In the case of the double plasmon resonance, when the resonant frequencies in the film and in the NP/film system coincide, *REF* can reach huge values close to 10^{13} .

An important goal in TERS would be to obtain single molecule sensitivity. The cross section of the non resonant Raman effect is typically in the order of 10^{-30} cm². For single molecule sensitivity a cross section in the order of 10^{-16} cm² is required as is well known from single molecule fluorescence studies. For single molecule TERS based solely on an electromagnetic enhancement a *REF* of 10^{14} would therefore be necessary [3, 4]. Our calculations show that such a factor can almost be reached in a configuration of an extended nanoparticle above a metal film, provided that the Raman dipole and the electric field at the dipole position are oriented along the symmetry axis and the NP/film gap is ~ 1 nm.

Acknowledgement

P. Geshev acknowledges support from the German Science Council (DFG). We also acknowledge support from the virtual institute "Functional properties of aquatic interfaces" of the Helmholtz Association of National Research Centers, Bonn, Germany, and from the European Network of Excellence, PLASM-NANO-DEVICES (FP6-2002-IST-1-507879).